# Measurements of the Electric Quadrupole Moment of Nb and Zr Isotopes with Modulated Adiabatic Fast Passage after Recoil Implantation into hcp Co

G. Seewald, E. Hagn, and E. Zech
*Physik Department, Technische Universität München, D-85748 Garching, Germany*

I. P. Johnstone and I. S. Towner
*Physics Department, Queen's University, Kingston, Ontario K7L 3N6, Canada*

D. Forkel-Wirth
*PPE Division, CERN, CH-1211, Geneva 23, Switzerland*

ISOLDE Collaboration
*CERN, CH-1211, Geneva 23, Switzerland*
(Received 30 July 1997)

We report a new method for the measurement of quadrupole moments of radioactive nuclei which were not accessible with other techniques until now: modulated adiabatic fast passage on oriented nuclei (MAPON) after recoil implantation into hcp Co. Quadrupole moments of Zr and Nb isotopes were determined which are interesting in the context of the proton and the neutron effective charge at $A \sim 90$. [S0031-9007(97)05107-7]

PACS numbers: 21.10.Ky, 76.60.Gv, 76.80.+y

Electric quadrupole moments of nuclear states are a measure for the nonsphericity of the electric charge density, which may originate from single-particle and collective nuclear properties. Thus, measurements of electric quadrupole moments may yield essential nuclear structure information. The standard method for the measurement of electric quadrupole moments of radioactive nuclei is laser spectroscopy (LS). Until now, the application of LS has been restricted mainly to nonrefractory elements. This is due to the fact that at on-line mass separators—such as ISOLDE at CERN—radioactive ion beams with high intensity are available only for nonrefractory elements. For only selected systems, laser desorption of daughter isotopes—which are not available in a primary beam—has been applied successfully; see, e.g., Ref. [1]. In recent years, diverse attempts have been started to improve the intensities of refractory elements at mass separators, such as the use of He-jet systems after nuclear reactions [2] or the development of on-line laser ion sources [3]. However, the intensities as obtained until now are still relatively small. Therefore another method would be desirable, with which quadrupole moments of radioactive nuclei can be measured, independent of the fact whether or not these are refractory. Here we introduce such a method, which is applicable to all elements throughout the nuclear chart: modulated adiabatic fast passage on oriented nuclei (MAPON) after recoil implantation into hcp-Co single crystals. The MAPON technique was introduced by Callaghan *et al.* [4,5]. It allows the determination of quadrupole splittings which are small in comparison to the magnetic inhomogeneous broadening. The power of the MAPON technique has not been recognized for long. This is due to the fact that mostly polycrystalline Fe had been used as host lattice for MAPON measurements. Because of the cubic symmetry the quadrupole interaction—it originates from an unquenched orbital momentum—is small. In addition, it is inhomogeneously broadened, the broadening being of the same order of magnitude as the total splitting. This is due to the fact that, as detected recently [6], the electric field gradient (EFG) at the impurity site in Fe depends strongly on the direction of magnetization with respect to the crystallographic axes. Therefore single crystal hcp Co as host lattice was supposed to be superior: The EFG originating from the noncubic lattice symmetry is well defined and, in addition, much larger than the EFG in Fe. In this case, however, the radioactive nuclei have to be implanted. With mass-separator implantation there exists the restriction to nonrefractory elements. If, however, recoil implantation after nuclear reactions was possible with single-crystal hcp Co this restriction should no longer apply, and the method should be applicable to all elements of the nuclear chart.

The technique of recoil implantation into hcp Co after nuclear reactions implies the use of thin Co single crystals in order to keep the amount of contaminant activities produced in Co small. Starting from a bulk hcp-Co single crystal available commercially, disks with a diameter of $\sim$10 mm and a thickness of $\sim$0.2 mm were cut off, the single crystal $c$ axis being oriented parallel to the surface. By a sophisticated procedure of mechanical abrading, chemical polishing steps, and finally electropolishing, the thickness could be reduced to $\sim$4 $\mu$m, with a success rate of $\sim$30%. With such crystals recoil-implantation experiments should be possible. However, it could not be anticipated *a priori* whether

 0031-9007/98/80(5)/924(4)$15.00 

radiation damage would deteriorate the long-range regular hexagonal lattice structure, which is necessary for a high resolution of the quadrupole interaction.

In this Letter we show that recoil implantation into hcp Co after $\alpha$-induced nuclear reactions is possible and that radiation damage represents no limiting factor.

The quadrupole moments of nuclei in closed-shell regions depend dominantly on single-particle properties; the polarizing effects of the valence nucleons on the nuclear core are included through the use of effective charges $e_{\mathrm{eff}}$. These effective charges may be determined experimentally from static electric quadrupole moments $Q$ or via transition $B(E2)$ values. The determination via $B(E2)$ values is normally less precise as two states are involved for which a detailed knowledge of the wave functions is necessary. For the $A \sim 90$ region, Raghavan *et al.* [7] measured quadrupole moments of the high-spin $8^+$ yrast states in $^{88}$Zr and $^{90}$Zr, which can be described within the shell model by a relatively pure $|(\pi g_{9/2})^{+2}\rangle_{8^+}$ ($^{90}$Zr) and $|(\nu g_{9/2})^{-2}\rangle_{8^+}$ ($^{88}$Zr) configuration. The sign of these quadrupole moments were determined by Bendahan *et al.* [8]. The result, $Q(^{88}\mathrm{Zr}; 8_1^+) = +0.51(3)$ b and $Q(^{90}\mathrm{Zr}; 8_1^+) = -0.51(3)$ b indicates that, within the experimental accuracy, the proton and neutron effective charge is nearly the same. Shell model calculations, taking $e_{\mathrm{eff}}^{(\pi)} = +2.0$ e and $e_{\mathrm{eff}}^{(\nu)} = +1.8$ e, yielded $+0.516$ b and $-0.504$ b for these states [7], respectively; i.e., the experimental data were well explained. More recently, shell model calculations of the quadrupole moments of the $8_1^+$ and $8_2^+$ states in $_{40}$Zr and $_{42}$Mo for $44 \leq N \leq 50$ were published by Weiszflog *et al.* [9]. Taking $e_{\mathrm{eff}}^{(\pi)} = +1.72$ e and $e_{\mathrm{eff}}^{(\nu)} = +1.44$ e, they also found that near $N = 50$ the quadrupole moments of the $|(\pi g_{9/2})^{+2}\rangle_{8^+}$ and $|(\nu g_{9/2})^{-2}\rangle_{8^+}$ states have opposite sign, but the quadrupole moments of the $|(\nu g_{9/2})^{-2}\rangle_{8^+}$ states should be considerably smaller. Thus an experiment would be desirable which is sensitive on the difference of the proton and neutron effective charge for $A \sim 90$. Here a measurement of the electric quadrupole moment of $^{90}$Nb ($I^\pi = 8^+$; $T_{1/2} = 14.6$ h) could serve: As the principal shell model configuration of this state is $|(\pi g_{9/2})^1(\nu g_{9/2})^{-1}\rangle_{8^+}$, the proton and neutron-hole contributions to the quadrupole moment nearly cancel. Thus the quadrupole moment is expected to be very small and reflects directly the difference of the proton and neutron effective charges. Measurements of other quadrupole moments among the Zr and Nb isotopes could be helpful to constrain the values of the effective charges to use in shell model calculations.

The $^{90}$Nb$\underline{\mathrm{Co}}^{(\mathrm{hcp})}$ sample was prepared at the cyclotron in Karlsruhe. A 4-$\mu$m Co single crystal with a 1.5 $\mu$m $^{90}$Zr foil in front of it was irradiated for 10 h with 55 MeV $\alpha$ particles. In this way $^{90}$Nb is produced via the nuclear reaction $^{90}\mathrm{Zr}(\alpha, 4n)^{90}\mathrm{Mo} \rightarrow {}^{90}\mathrm{Nb}$ and a sufficient amount of $A = 90$ atoms is implanted into Co (implantation depth $\sim 0.2$ $\mu$m).

After the irradiation the sample was cooled to temperatures $\sim 10$ mK with a $^3$He-$^4$He-dilution refrigerator. The $\gamma$ rays emitted in the decay of $^{90}$Nb were detected with 4 Ge detectors placed at 0°, 180°, and 90°, 270° with respect to the single-crystal $c$ axis. The $\gamma$ anisotropy $\epsilon = W(0°)/W(90°) - 1$—here $W(\vartheta)$ is the angular distribution of $\gamma$ rays emitted in the decay of oriented nuclei [10]—of the 141, 1129, and 2319 keV $\gamma$ transitions was analyzed. First a standard NMR on oriented nuclei (NMR-ON) experiment was performed; the resonance was found at $\overline{\nu} = 81.87(1)$ MHz, with a half-width $\Gamma = 0.52(4)$ MHz. The ratio $\overline{\nu}/\Gamma = 157(12)$ indicates a high quality of the hexagonal structure of the sample. No resonance signal was observed around 71.8 MHz, which is known to be the magnetic hyperfine interaction frequency of $^{90}$Nb in fcc Co [11].

For the determination of the quadrupole interaction, which is completely invisible in the NMR-ON spectrum, a MAPON measurement was performed. The principle of MAPON is described in detail in Refs. [4,5]. MAPON is a variant of adiabatic fast passage (AFP) in which the rf frequency is slowly and continuously swept through the resonance conditions. With AFP on a quadrupole split system, cyclic permutation of the subresonance population probabilities $a_m$ is obtained. A MAPON pulse consists of a sequence of *two* AFP pulses which are separated in frequency by $\Delta\nu$. The influence of the MAPON pulse on the time evolution of the sublevel populations is different for $\Delta\nu > \Delta\nu_Q$ and $\Delta\nu < \Delta\nu_Q$, where $\Delta\nu_Q$ is the quadrupole subresonance separation,

$$\Delta\nu_Q = 3\nu_Q/[2I(2I-1)], \tag{1}$$

$$\nu_Q = eQV_{zz}/h. \tag{2}$$

Here $I$ is the nuclear spin, $eQ$ is the spectroscopic quadrupole moment, and $V_{zz}$ is the principal component of the EFG tensor. (i) For $\Delta\nu > \Delta\nu_Q$ the MAPON pulse causes a distinctive reorganization of sublevel populations in which a net population transfer of the first *two* accessed substate populations is cyclically permuted through to the final two substates. (ii) For $\Delta\nu < \Delta\nu_Q$ the successive double transits through each subresonance yield a null result. The different sublevel populations $a_m$ in these two cases cause different $\gamma$ anisotropies, and $\Delta\nu_Q$ is obtained from the transition between the respective $\gamma$ anisotropy values. The MAPON spectrum of $^{90}$Nb$\underline{\mathrm{Co}}^{(\mathrm{hcp})}$ is shown in Fig. 1; the results are listed in Table I. We want to point out that the sign of the quadrupole interaction can be determined uniquely, either with MAPON or AFP. In both cases it is obtained immediately from the time dependence of the postpassage signal.

For the determination of the quadrupole moment from the measured quadrupole interaction frequency the EFG has to be known. This can be obtained via MAPON measurements on an isotope for which the quadrupole moment is known—there is no such case for Nb—or can be predicted moderately well in the framework of

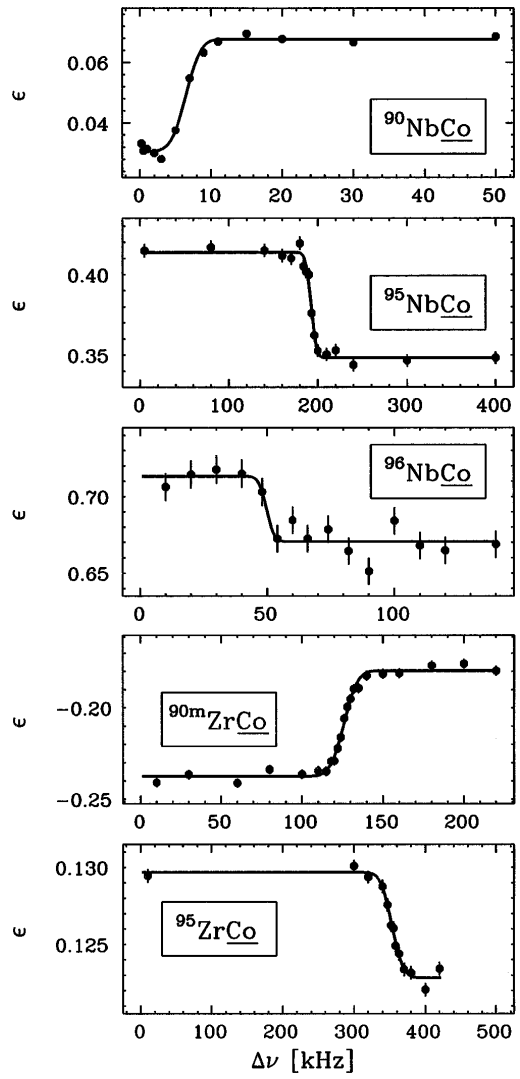


FIG. 1. MAPON spectra of $^{90,95,96}$Nb and $^{90}$Zr$^{m}$, $^{95}$Zr in hcp Co. The solid lines are the results of least-squares fits, taking into account a Gaussian distribution for the quadrupole subresonance resonance separation with center at $\Delta\nu_Q$ and width $\Gamma_{\Delta\nu_Q}$. The MAPON signal is given by the integral of this distribution, i.e., an error function with the half value at $\Delta\nu_Q$ and width $\Gamma_{\Delta\nu_Q}$. The different sign of the MAPON signals of $^{95,96}$Nb and $^{95}$Zr in comparison to $^{90}$Nb and $^{90}$Zr$^{m}$ is due to the fact that the $\gamma$ anisotropy of $^{95,96}$Nb and $^{95}$Zr is positive, whereas it is negative for $^{90}$Nb and $^{90}$Zr$^{m}$.

nuclear-model calculations. In the present case $^{95}$Nb and $^{96}$Nb were viewed to be suitable as it was supposed that the quadrupole moments of $^{95}$Nb and $^{96}$Nb can be predicted more reliably by shell model calculations than the quadrupole moment of $^{90}$Nb.

A $^{95}$Nb$\underline{\text{Co}}^{(\text{hcp})}$ sample was prepared by mass separator implantation at ISOLDE at CERN. $^{95}$Rb was implanted with $E = 60$ keV into a hcp-Co single crystal with high surface quality (total dose $\sim 10^{12}$). The following decay chain is relevant: $^{95}$Rb ($T_{1/2} = 0.38$ s) $\rightarrow$ $^{95}$Sr ($T_{1/2} = 24$ s) $\rightarrow$ $^{95}$Y ($T_{1/2} = 10$ min) $\rightarrow$ $^{95}$Zr ($T_{1/2} = 64.0$ d) $\rightarrow$ $^{95}$Nb ($T_{1/2} = 35.0$ d). First a NMR-ON experiment was performed. The results are $\overline{\nu} = 179.39(4)$ MHz and $\Gamma = 0.72(8)$ MHz. The ratio $\overline{\nu}/\Gamma = 250(28)$ indicates a slightly higher quality of the sample in comparison to $^{90}$Nb. A MAPON spectrum is shown in Fig. 1; the results are listed in Table I.

For the preparation of the $^{96}$Nb$\underline{\text{Co}}^{(\text{hcp})}$ sample the recoil-implantation technique was applied, utilizing the reaction $^{96}$Zr$(\alpha, 3np)^{96}$Nb ($E_\alpha = 65$ MeV). Here the NMR-ON resonance was found at $\overline{\nu}(B_{\text{ext}} = 1\ \text{kG}) = 108.42(4)$ MHz, with a half-width $\Gamma = 0.44(18)$ MHz. The ratio $\overline{\nu}/\Gamma = 250(100)$ indicates a similar quality of the sample in comparison to $^{90}$Nb and $^{95}$Nb. A MAPON spectrum is shown in Fig. 1; the results are listed in Table I.

For Zr, NMR-ON and MAPON measurements were performed on $^{90}$Zr$^{m}$ ($I^\pi = 5^-$; $T_{1/2} = 0.8$ s; configuration $|(\pi g_{9/2})^1(\pi p_{1/2})^1\rangle_{5^-}$) and $^{95}$Zr ($I^\pi = 5/2^+$; $T_{1/2} = 64.0$ d). The MAPON spectra are shown in Fig. 1; the results are listed in Table I.

The quadrupole interaction frequencies are summarized in Table II, together with theoretical quadrupole moments calculated within the framework of the nuclear shell model (column 5). These quadrupole moments were calculated using a $^{88}$Sr core, with protons and neutron holes in the $p_{1/2}$ and $g_{9/2}$ shells. Neutrons for $N > 50$ were allowed to occupy the $d_{5/2}, s_{1/2}, d_{3/2}$, and $g_{7/2}$ shells, with up to two neutrons out of the $d_{5/2}$ shell. For $^{90}$Nb, the interaction used was the interaction of Serduke, Lawson, and Gloeckner [14], while for $^{95}$Zr, $^{95}$Nb, and $^{96}$Nb it was the JS6 interaction of Johnstone and Skouras [15]. The $5^-$ state of $^{90}$Zr was assumed to have a $p_{1/2}g_{9/2}$ proton configuration. Proton and neutron effective charges from a recent calculation by Towner and Johnstone [16], given in Table III, are significantly different for $^{88}$Sr and $^{90}$Zr cores, due to the large contributions from $p_{3/2} \rightarrow p_{1/2}$ and $f_{5/2} \rightarrow p_{1/2}$ proton excitations. This was taken into account in the calculations by using different effective charges for wave function

TABLE I. Results of the MAPON measurements. The ratio $|\Delta\nu_Q|/\Gamma_{\Delta\nu_Q}$ is a measure for the sharpness of the quadrupole interaction.

| Isotope | $I^\pi$ | $\Delta\nu_Q$ (kHz) | $\Gamma_{\Delta\nu_Q}$ (kHz) | $\lvert\Delta\nu_Q\rvert/\Gamma_{\Delta\nu_Q}$ | $\nu_Q$ (MHz) |
|---|---|---|---|---|---|
| $^{90}$Nb | $8^+$ | −6.4(3) | 4.0(6) | 1.6(3) | −0.512(24) |
| $^{95}$Nb | $9/2^+$ | +193.2(5) | 6(2) | 34(9) | +4.637(12) |
| $^{96}$Nb | $6^+$ | +50(2) | 6(6) | 8(8) | +2.20(9) |
| $^{90}$Zr$^{m}$ | $5^-$ | +126(2) | 16(1) | 7.9(5) | +3.78(6) |
| $^{95}$Zr | $5/2^+$ | −353(1) | 29(5) | 12(2) | −2.353(7) |

TABLE II. Quadrupole interaction frequencies and quadrupole moments of Nb and Zr isotopes. The sign of the quadrupole interaction was determined experimentally in all cases.

| Isotope | $I^\pi$ | $\nu_Q$ (MHz) | $Q_{\text{expt}}$ (b) | $Q_{\text{theor}}$ (b) |
|---|---|---|---|---|
| $^{90}$Nb | $8^+$ | $-0.512(24)$ | $+0.046(7)$[a] | $+0.04$ |
| $^{93}$Nb | $9/2^+$ | | $-0.32(2)$[b] | $-0.38$ |
| | | | $-0.366(18)$[c] | |
| $^{95}$Nb | $9/2^+$ | $+4.637(12)$ | | $-0.40$ |
| $^{96}$Nb | $6^+$ | $+2.20(9)$ | | $-0.23$ |
| $^{90}$Zr$^m$ | $5^-$ | $+3.78(6)$ | | $-0.35$ |
| $^{91}$Zr | $5/2^+$ | | $-0.206(10)$[c] | $-0.20$ |
| $^{95}$Zr | $5/2^+$ | $-2.353(7)$ | $+0.22(2)$[d] | $+0.23$ |

[a] Derived with the ratio $\nu_Q(^{90}\text{Nb})/\nu_Q(^{95}\text{Nb})$ and taking into account a 15% uncertainty of the theoretical $Q(^{95}\text{Nb})$.
[b] Muonic x-ray spectroscopy, Ref. [12].
[c] Atomic beam magnetic resonance, Ref. [13]; no Sternheimer correction included.
[d] Derived with the ratio $\nu_Q(^{95}\text{Zr})/\nu_Q(^{90}\text{Zr}^m)$ and taking into account a 10% uncertainty of the theoretical $Q(^{90}\text{Zr}^m)$.

components with an empty $p_{1/2}$ shell than for components with a filled $p_{1/2}$ shell. The proton $p_{1/2}$ shell is half filled in $^{90}\text{Zr}(5^-)$ and in some components of $^{90}\text{Nb}(8^+)$; for these, an average effective charge was used.

Taking the theoretical quadrupole moment for $^{95}$Nb and assuming a 15% uncertainty—the maximal uncertainty is estimated by comparing the theoretical and experimental quadrupole moments for $^{93}$Nb (see Table II)—we can calibrate the EFG of Nb$\underline{\text{Co}}$, with the result $V_{zz}(\text{Nb}\underline{\text{Co}}^{(\text{hcp})}) = -0.48(7) \times 10^{17}$ V/cm$^2$. With the experimental ratio $\nu_Q(^{90}\text{Nb})/\nu_Q(^{95}\text{Nb}) = -0.110(5)$ the quadrupole moment of $^{90}$Nb is deduced to be

$$Q(^{90}\text{Nb}; 8^+) = +0.046(7)\ \text{b}.$$

This small result displays the nearly complete cancellation between the neutron and proton contributions and agrees well with the theoretical calculation [16] based on the effective charges of Table III. A further test of the shell model can be achieved using a similar analysis among the Zr isotopes. With our measured ratio of frequencies $\nu_Q(^{95}\text{Zr})/\nu_Q(^{90}\text{Zr}^m) = -0.623(10)$ and a shell model calculation of $Q(^{90}\text{Zr}^m)$, to which we assign a 10% uncertainty, we derive the result $Q(^{95}\text{Zr}) = +0.22(2)$ b, in excellent agreement with theory. The EFG is deduced to be $V_{zz}(\text{Zr}\underline{\text{Co}}^{(\text{hcp})}) = -0.45(5) \times 10^{17}$ V/cm$^2$.

TABLE III. Calculated proton and neutron effective charges $e_{\text{eff}}^{(\pi)}$ and $e_{\text{eff}}^{(\nu)}$.

| | $p_{1/2}$ shell | |
|---|---|---|
| | Filled | Empty |
| $e_{\text{eff}}^{(\pi)}(g_{9/2} \rightarrow g_{9/2})$ | 1.718 | 2.115 |
| $e_{\text{eff}}^{(\nu)}(g_{9/2} \rightarrow g_{9/2})$ | 1.234 | 1.951 |
| $e_{\text{eff}}^{(\nu)}(s_{1/2} \rightarrow d_{3/2})$ | 0.774 | 1.032 |
| $e_{\text{eff}}^{(\nu)}(s_{1/2} \rightarrow d_{5/2})$ | 0.792 | 1.079 |
| $e_{\text{eff}}^{(\nu)}(d_{3/2} \rightarrow d_{3/2})$ | 0.872 | 1.349 |
| $e_{\text{eff}}^{(\nu)}(d_{3/2} \rightarrow d_{5/2})$ | 0.925 | 1.398 |
| $e_{\text{eff}}^{(\nu)}(d_{3/2} \rightarrow g_{7/2})$ | 0.910 | 1.196 |
| $e_{\text{eff}}^{(\nu)}(d_{5/2} \rightarrow d_{5/2})$ | 0.880 | 1.402 |
| $e_{\text{eff}}^{(\nu)}(d_{5/2} \rightarrow g_{7/2})$ | 0.927 | 1.306 |
| $e_{\text{eff}}^{(\nu)}(g_{7/2} \rightarrow g_{7/2})$ | 1.261 | 1.917 |

Summarizing, with MAPON after recoil implantation into hcp Co we have introduced a new method for the precise measurement of the quadrupole interaction of radioactive nuclei, from which precise ratios of quadrupole moments can be deduced. There are no restrictions to nonrefractory elements. It has a wide applicability to all radioactive isotopes which can be produced by a suitable nuclear reaction.

We wish to thank Dr. J. Völkl, W. Clauß, G. Neff, H. Schneider, M. Stanger, and H. Utz of the Kristall-Labor for the preparation of the Co single crystals, and E. Smolic for experimental help. This work has been funded by the Deutsche Forschungsgemeinschaft (DFG) under Contract No. Ha 1282/3-3, and, partly, by the Forschungszentrum Karlsruhe.

[1] F. Le Blanc *et al.*, Phys. Rev. Lett. **79**, 2213 (1997).
[2] J. Ärje, J. Äystö, H. Hyvönen, P. Taskinen, V. Koponen, J. Honanken, A. Hautojärvi, and K. Vierinen, Phys. Rev. Lett. **54**, 99 (1985).
[3] L. Vermeeren *et al.*, Phys. Rev. Lett. **73**, 1935 (1994).
[4] P. T. Callaghan, P. J. Back, D. H. Chaplin, H. R. Foster, and G. V. H. Wilson, in *Proceedings of the International Symposium on Nuclear Orientation and Nuclei far from Stability* [Hyperfine Interact. **22**, 39 (1985)].
[5] P. T. Callaghan, P. J. Back, and D. H. Chaplin, Phys. Rev. B **37**, 4900 (1988).
[6] G. Seewald, E. Hagn, E. Zech, D. Forkel-Wirth, A. Burchard, and ISOLDE Collaboration, Phys. Rev. Lett. **78**, 1795 (1997).
[7] P. Raghavan, M. Senba, Z. Z. Ding, A. Lopez-Garcia, B. A. Brown, and R. S. Raghavan, Phys. Rev. Lett. **54**, 2592 (1985).
[8] J. Bendahan, C. Broude, E. Dafni, G. Goldring, M. Hass, E. Naim, and M. H. Rafailovich, Phys. Rev. C **33**, 1517 (1986).
[9] M. Weiszflog, J. Billowes, J. Eberth, C. J. Gross, M. K. Kabadiyski, K. P. Lieb, Y. Mylaeus, and D. Rudolph, Nucl. Phys. **A584**, 133 (1995).
[10] K. S. Krane, in *Low-Temperature Nuclear Orientation*, edited by N. J. Stone and H. Postma (North-Holland, Amsterdam, 1986), p. 31.
[11] E. Hagn, E. Zech, and G. Eska, J. Phys. F **12**, 1475 (1982).
[12] H. P. Povel, Nucl. Phys. **A217**, 573 (1973).
[13] S. Büttgenbach, *Hyperfine Structure in 4d- and 5d-Shell Atoms*, Springer Tracts in Modern Physics Vol. 96 (Springer-Verlag, Berlin, 1982).
[14] F. J. D. Serduke, R. D. Lawson, and D. H. Gloeckner, Nucl. Phys. **A256**, 45 (1976).
[15] I. P. Johnstone and L. D. Skouras, Phys. Rev. C **51**, 2817 (1995).
[16] I. S. Towner and I. P. Johnstone (unpublished); Queen's University report, 1997.